Air quality, metal(loid) sources identification and environmental assessment using (bio)monitoring in the former mining district of Salsigne (Orbiel valley, France)

Aude Calas, Eva Schreck, Jérôme Viers, Astrid Avellan, Alain Pages, Maria Dias-Alves, Eric Gardrat, Philippe Behra, Véronique Pont

Air quality, metal(loi)d sources identification and environmental assessment using (bio)monitoring in the former mining district of Salsigne (Orbiel valley, France)

Aude CALAS[1,2,*], Eva SCHRECK[1], Jérôme VIERS[1], Astrid AVELLAN[1], Alain PAGES[3], Maria DIAS-ALVES[4], Eric GARDRAT[4], Philippe BEHRA[2] and Véronique PONT[4]

[1] Géosciences Environnement Toulouse (GET), Université de Toulouse, CNRS, IRD, 14 Avenue Edouard Belin, 31400, Toulouse, France.

[2] Laboratoire de Chimie Agro-industrielle (LCA), Université de Toulouse, INRAE, Toulouse INP, Toulouse, France.

[3] Observatoire Midi-Pyrénées, 16 avenue Edouard Belin 31400 Toulouse, France.

[4] Laboratoire d'Aérologie, Université de Toulouse, CNRS, 14 Avenue Edouard Belin, 31400, Toulouse, France.

*Corresponding author: Aude Calas; aude.calas@get.omp.eu ; aude.calas@toulouse-inp.fr

Abstract

The former mining district of Salsigne is situated in the Orbiel valley. Until the 20th century, it was the first gold mine in Europe and the first arsenic mine in the world. Rehabilitation has been performed during the 20 years that followed closure of the mines and factories, which led to the accumulation of storage of several million tons of waste in this valley. Nevertheless, a detailed description of the air quality of this area is still missing. The goal of the present study is to evaluate atmospheric contamination in the valley and identify the potential sources of this contamination.

Active monitors (particulate matter samplers) and passive bioindicators (*Tillandsia usneoides*) were placed in strategic sites including remote areas. Over the year 2022, we assessed the air quality using microscopic and spectroscopic techniques, as well as environmental risk indicators to report the level of contamination.

Results indicate that the overall air quality in the valley is good with PM_{10} levels in accordance with EU standards. Elemental concentrations in the exposed plants were lower than reported in the literature. Among the different sites studied, Nartau and La Combe du Saut, corresponding to waste storage and former mining industry sites, were the most affected. Chronic exposure over 1 year was highlighted for Fe, Ni, Cu, Pb, Sb and As. Pollution Load Index and Enrichment Factors, which provided valuable information to assess the environmental condition of the valley's air, suggested that dust and resuspension of anthropogenic materials were the principle sources for most of the elements. Finally, this study also highlights that using *T. usneoides* could be a convenient approach for biomonitoring of metal(loid)-rich particles in the atmosphere within a former mining area, for at least one year. These results in turn allow to better understand the effects of chronic exposure on the ecosystem.

Highlights

- In 2022, the Orbiel valley air quality was in compliance with regulations
- Dust and anthropogenic resuspensions were the principal sources of metal(loid)s
- NRT and CDS sites were identified to be the most contaminated sites
- Except Cu and Zn, all elements showed linear deposition kinetics on *T. usneoides*

Graphical Abstract

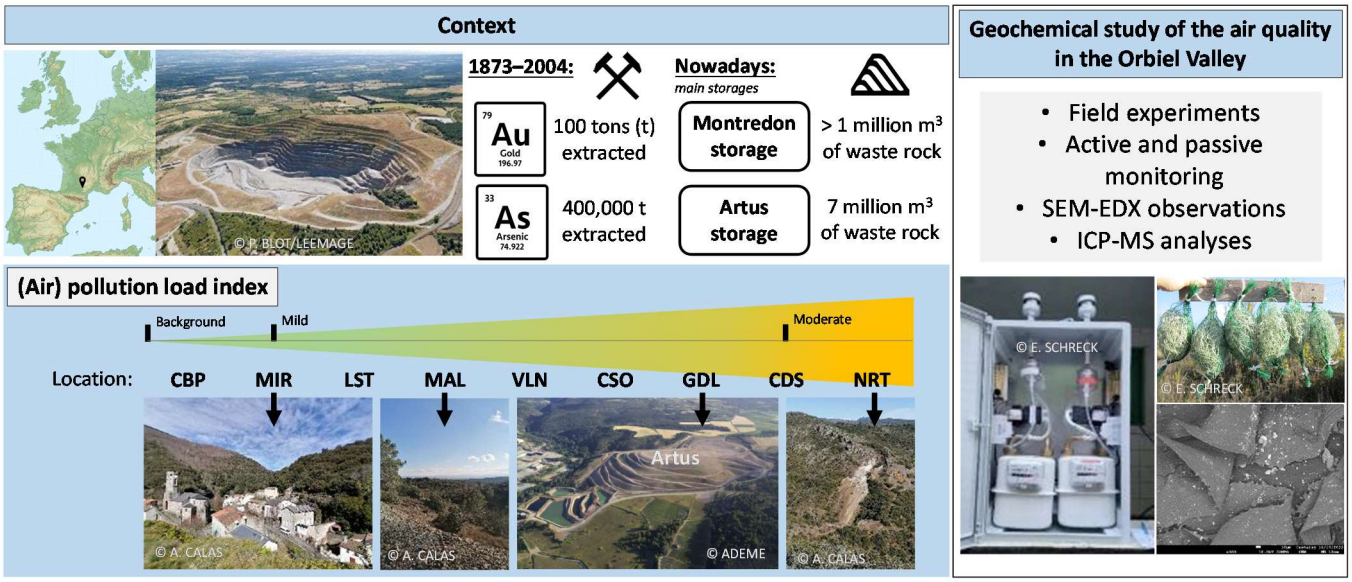

1. Introduction

Mining activities contribute significantly to toxic metal(loid) contaminants in the environment, which persist long (even decades) after mine closure (Delplace et al., 2022). The different environmental components, i.e., surface and groundwater, soil, sediment, atmosphere and biosphere, typically bear this impact (Bondu et al., 2023; Chen et al., 2017; Delplace et al., 2022; Elbaz-Poulichet et al., 2017; Huertas et al., 2012; Tepanosyan et al., 2018). In southern France, the border region of the Massif Central has long served as a major mining area for non-ferrous (Pb-Zn-Ag-Au) metals dating back to at least the medieval period and probably even as early as the Roman period (Elbaz-Poulichet et al., 2017). In the late 19th century, following the discovery of Au ores, mining activities were intensified and continued up until the second half of the 20th century, after which they gradually decreased (Elbaz-Poulichet et al., 2017). Located on the south-western terminus of the Massif Central area, the Orbiel valley, more precisely, the Salsigne old mining district, includes various sites that are linked to former (ore extraction and processing) and current mining activities (waste storage). The main mine was, at some point in the 20th century, the first Au mine in Europe and the first As mine in the world. In the period following the discovery of Au in 1892 until the closure of the mine in 2004, around 120 t of Au were produced, the highest output of any Au mine in Western Europe. From 1873 to 1910, about 25% of the world's As needs were supplied by this mine (Drouhot et al., 2014; Trueb, 1996). However, as indicated by the various mining concessions, there were several other secondary mines in this area (Figure 1 top map), covering a total surface area of 39.78 km² (Vermeersch et al., 2012). Ore processing, which historically was conducted close to the extraction sites, was later relocated to the central processing area of La Combe du Saut (Desaulty et al., 2016). After the closure of the different mines and factories, a rehabilitation of the area was undertaken and carried out over a span of 20 years with several million t of waste stored in the valley. The main waste storages are located at the sites of Montredon (> 1 million m^3 of waste rock), Artus (7 million m^3 of waste rock), and La Combe du Saut (Rochereau et al., 2021). The Montredon storage (MRD) area, while mainly containing waste from the cyanidation of ores, also has flotation residues, lime arsenates, residues from the Malabau

concession, and sewage sludge. The Artus storage (ART) area also serves as a repository for waste from the cyanidation of the ore and flotation residues but unlike Montredon, this storage site neither has a bottom seal nor does it have a waterproof covering system (Desaulty et al., 2016). Finally, the wastes produced from the demolition of factory buildings and pyrometallurgical slag are the main wastes stored in geomembranes at La Combe du Saut (CDS) (Desaulty et al., 2016; Drouhot et al., 2014). Other waste rock piles located in the valley include the waste pile of Nartau (NRT), the waste pile of Malabau (MAL) (45 000 m^3), (Vermeersch et al., 2012), the waste storage of La Caunette (CAU), or the waste piles surrounding the open-mine of Salsigne (SAL, RML) (Figure 1).

The most recent extreme precipitations and flood events, (October 2018, categorized as a 100-year flood) have brought to light the mining history of the area and have raised concerns among a certain segment of the inhabitants in the valley regarding their immediate environment.

Recent studies have revealed the contamination by metals and metalloids, particularly of As, due to anthropogenic activities, of surface and groundwaters (Heydon et al., 2023; Khaska et al., 2015), sediments (Delplace et al., 2022), and also As transfer to wild small mammals (Drouhot et al., 2014).

Furthermore, since 1997, prefectural decrees, starting with the publication of the first decree concerning vegetable sales, have been issued, prohibiting the sale of certain vegetables grown in the Orbiel valley or the utilization of water from the Orbiel river and its tributaries. However, despite numerous studies on the various environmental components, there have been only few studies on the levels of atmospheric pollution in this impacted valley (Bausch and Merlen, 2021; Durif et al., 2006). This is all the more relevant because, the World Health Organization (WHO) has estimated that every year, exposure to ambient air pollution causes millions of deaths and the loss of healthy years of life (World Health Organization, 2021). In the past, mining activities were assumed to be major sources of toxic elements such as As in the atmosphere, in the form of aerosols and gas, from the mine and the extraction plants in the Orbiel valley. It is noted here that there have been no peer-reviewed studies to assess air quality in this rural and windy valley since mining operations ceased. There are however, two technical reports by the French Geological Survey (BRGM), responsible for the rehabilitation of

the mining sites of the area (Bausch and Merlen, 2021; Durif et al., 2006). The valley has a typically continental climate with a blend of Mediterranean and oceanic influences featuring a relatively high annual rainfall (900 mm) combined with a mild annual average temperature (13 °C) (Delplace et al., 2022). Additionally, the valley also frequently experiences strong winds (average values in Carcassonne from 1991 to 2022: 98.5 d/y with wind speed > 16 m/s). Moreover, wind friction on surfaces such as the waste storage sites, has already been reported to contribute significantly to the emission and transport of metal(loid)-rich particles in mining areas. The potential impacts of these emissions on the environment and human health have been described (Blondet et al., 2019; Csavina et al. 2012; Sánchez de la Campa et al., 2011; Yulevitch et al., 2020; Zota et al., 2009).

In addition to traditionally used methods, several new approaches such as biomonitoring have been developed in recent years to monitor atmospheric quality. Biomonitoring methods include the use of bioindicators such as mosses, lichens, tree barks, tree rings, pine needles, grass, leaves and ferns (Figueiredo et al., 2007) but also the use of epiphytic bromeliads (i.e., *Tillandsia spp.*) that absorb water and nutrients directly from the atmosphere and are adapted to avoid hydric stress. These low-cost and easy-to-perform tools help to overcome technical constraints associated with field studies, such as lack of electricity or areas that do not have easy access, and to better assess air quality over larger and more remote areas. Among the *Tillandsia spp.*, *Tillandsia usneoides* has been reported to be a good bioindicator to detect metal contamination (Figueiredo et al., 2007; Isaac-Olivé et al., 2012; Martínez-Carrillo et al., 2010; Parente et al., 2023; Pellegrini et al., 2014; Schreck et al., 2020) and to identify the sources of contamination (dust, vehicular, industrial origin) (Figueiredo et al., 2007; Pellegrini et al., 2014) as reported in several recent studies, especially in South America. In these studies, the consecutive monitoring periods ranged from 15 days (Isaac-Olivé et al., 2012; Martínez-Carrillo et al., 2010) to 52 weeks (Schreck at al., 2020) but were usually shorter than 13 weeks. Notwithstanding, *T. usneoides* has rarely been used in Europe (Pellegrini et al., 2014; Schreck at al. 2020).

In this study, we conducted field experiments using active monitors such as PM samplers, while complementing them with passive bioindicators, specifically *T. usneoides*, in order to (i) assess the air

quality of the Orbiel valley over a one-year time period using traditional PM samplers as well as innovative plants-based tools in the more remote areas, (ii) identify potential sources of air contamination as well as the most impacted areas in the valley, (iii) assess the environmental status of the valley using pollution indexes from an atmospheric standpoint.

2. Material and methods

2.1. Study area and instrumentation

The main waste storage areas, namely, Montredon (MRD), La combe du Saut (CDS), and Artus (ART) are located in the villages of Salsigne, Lastours and Limousis, respectively, and situated at around 13 Km north of the city of Carcassonne (South France, Figure 1).

We selected nine strategic sites to assess the overall air quality in the selected area (Figure 1 bottom map, Table SI 1). Passive bioindicators such as *T.usneoides,* as well as the active monitors, PM_{10} collected on Teflon filters, were deployed in 4 sites: The **Gouffre de Cabrespine** (**CBP** – the control site without any past mining exploitation activity and located in the Clamoux valley), **Miraval-Cabardès** (**MIR** – a village in the upstream part of the Orbiel river characterized by minimal mining activities), **Lastours** (**LST** – another village situated downstream along the river and containing several mine galleries), and **La Combe du Saut** (**CDS** – formerly the main ore processing area but now mainly containing waste from the demolition of the plant buildings). The last site is also in proximity to La Caunette (CAU), a former ore processing and storage area, and the waste storage facility of Montredon (MRD). Today, "La Caunette" corresponds to an open quarry for aggregates located in the CAU concession.

Passive biomonitoring was extended to 5 sites, which allowed to better cover the valley and extend the study to rural areas and more remote sites such as, **Conques-sur-Orbiel** (**CSO** – town in the downstream part of the Orbiel river and without past mining activities), **Villanière** (**VLN** - 300 m from the waste rock pile of Cimetière south of the open-pit mine of Salsigne (SAL) and in proximity to the town of Villanière), **Malabau** (**MAL** – on the waste rock pile, a former ore extraction and processing site), **Nartau** (**NRT** –500 m from the waste rock pile of Nartau (NRT), a former ore extraction and processing site and at 600 m from the waste rock pile of Terrisse/Ramèle (RML) situated north-east of the open-pit mine of Salsigne (SAL), and **Gué de Lassac** (**GDL** - near the storage facility of Artus (ART)).

From the sites of MIR (north), to MAL (west), to CSO (south), to LST (east), the (bio)monitoring area represents 22 km², excluding the control site of CBP, in the Clamoux valley.

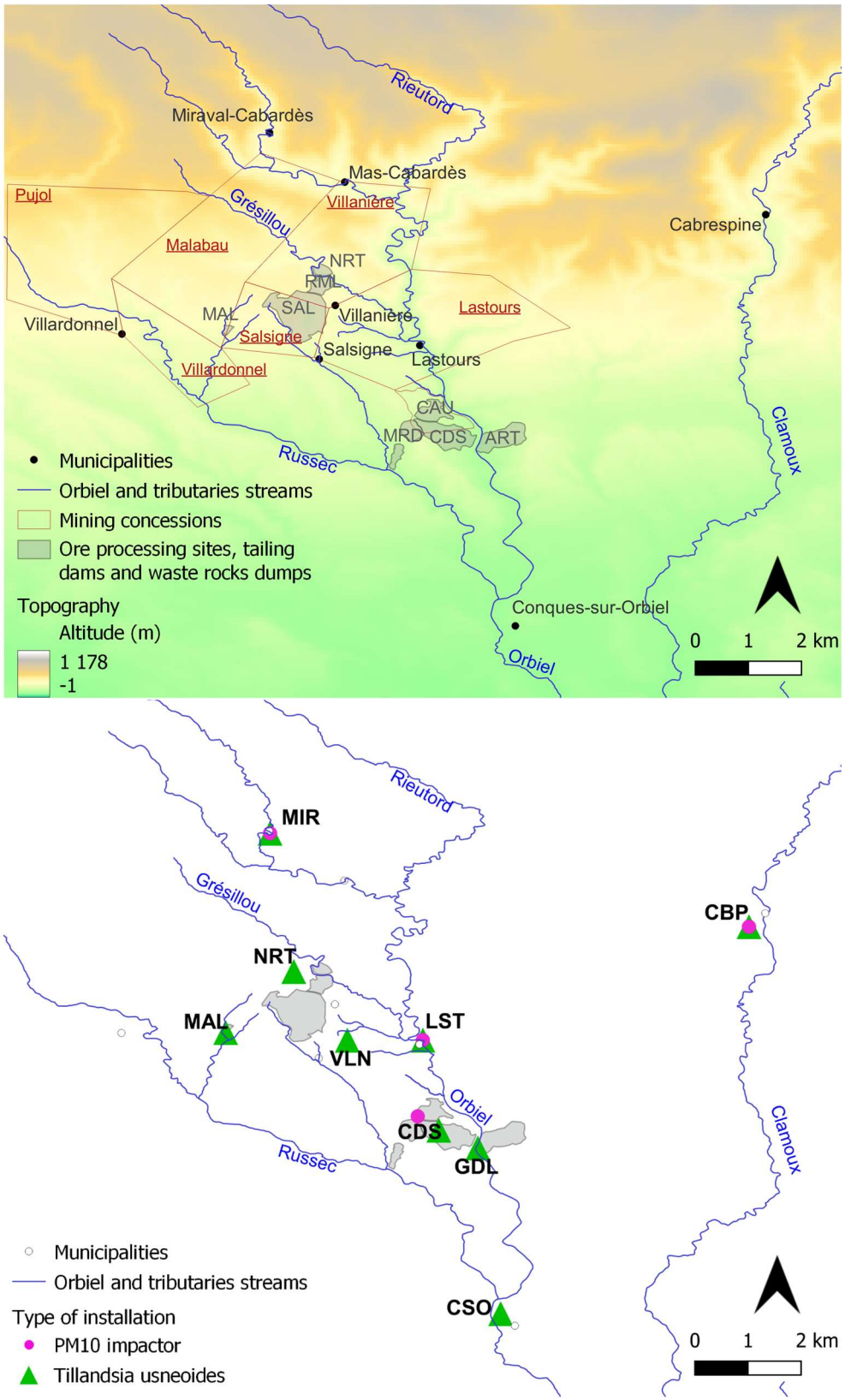

Figure 1: General context and sampling strategy. *Top map:* mining history of the Orbiel valley with topographic description. *Bottom map*: location of the sampling sites for atmospheric (bio)monitoring from October 2021 to December 2022, in the Orbiel valley (Aude, France); CBP = Gouffre de Cabrespine; MIR = Miraval; CSO = La Conques sur Orbiel; LST= Lastours; VLN = Villanière; MAL = Malabau; NRT = Nartau; GDL = Gué de Lassac; CDS = La Combe du Saut.

2.2. Abiotic parameters

Recordings of abiotic parameters, i.e. wind and precipitation, were used to better understand their influence on PM_{10} distribution in the environment. Synoptic wind variables, i.e. wind direction and speed at GPS point 43°20'52'' N, 2°23'29'' E, were extracted from *earth.nullschool.net*, based on forecasts and reanalysis from the Global Forecast System (GFS, EMC / NCEP / US National Weather Service). These data can be used to track large-scale atmospheric flows and were extracted daily at 12h00 and 700 hPa altitude. The wind direction most frequently observed over a period of 15 days was selected to represent the direction of maximum influence over the 15-integrated days of PM_{10} sampling. The median wind speed was calculated over the same 15-day period.

With regard to precipitation, the Integrated Multi-satEllite Retrievals algorithm of the international satellite mission Global Precipitation Measurement (GPM) was used to estimate precipitation in the Orbiel valley. The data were provided by Google Earth Engine, through the GPM v6 collection with a spatial resolution of 0.1°× 0.1° (roughly 10 km x 10 km) and a temporal resolution of 30 min (as used by de Fleury et al., 2023). The cumulative amount of precipitation was also calculated over the same 15-day period.

2.3. Experimental set-up and sampling

2.3.1. PM_{10} sampling for air composition study

Our choice to study PM_{10} was based on the fact that coarse particles were expected to be associated with waste storage areas, i.e. plant closure, potential particle emissions due to wind friction on surfaces. In December 2021, we installed PM_{10} impactors in 4 sites (see Figure 1 and Table SI 1). Aerosols were collected continuously on Teflon filters during 15-integrated sampling days, in the time period from December 2021 to December 2022. The PM_{10} impactors operated at a flow rate of 5 L min^{-1}. Samples of PM_{10} were collected on Teflon filters (Pall TF-45, 47 mm diameter and 0.45 µm cut off) to

characterise particulate trace metals and metalloids of interest. Teflon filters, including blanks, were weighed before and after sampling, and analysed for trace elements. Note that for the CDS site, sampling started 2 weeks after sampling in the other sites (January 2022).

2.3.2. Experimental set-up using *T. usneoides* as indicator to determine metal(loid) concentrations in the air

Plants of similar size were bought at Botanic® garden supplies store and washed with ultrapure water. The plants were then placed in nylon mesh bags containing one plant in each bag (Figure SI 1). In October 2021, in each of the 9 sites, 6 bags per site were secured on trees or wooden posts at a height of 1.7 m. At each of the sites, a plant was collected every 2 months in the time period between January and November 2022 to determine the kinetics of deposition (and potential uptake) of airborne particulate matter over a full year. After collection, the plants were dried at 45 °C for 48 – 72 h, ground in an agate mortar with liquid N_2, dried again if needed, and stored in polyethylene vials.

Additionally, 3 nylon mesh bags (containing 3 *T. usneoides*) were kept in the laboratory as controls (unexposed) in October 2021. In November 2021, these controls were dried, ground and analysed in an identical manner as the exposed *T. usneoides* samples. Following the methodology of Figueiredo et al. (2007), the plants were not washed after exposure because both deposition and potential uptake are considered in this study.

2.4. SEM-EDX observations of epiphytic plants

Environmental scanning electron microscopy with energy-dispersive X-ray spectroscopy (SEM-EDX) measurements were carried out on epiphytic plants at the Centre de Microcaractérisation Raimond Castaing in Toulouse (France), using a (FEG) JSM-7800F Prime (Jeol®) instrument equipped with EDX detector. SEM-EDX analyses were performed on unwashed *T. usneoides* exposed for 6 months in CDS,

to observe their morphology, trichome conformation, and the possible presence of metal(loid)s on the plant surface. Plants were dried and fixed on a carbon substrate and imaged as such.

2.5. Acidic mineralisation of samples and determination of elemental concentrations by ICP-MS

To determine the elemental composition of *T. usneoides*, 0.100 g of dry matter was digested using a mixture of 8 mL of bi-distilled HNO_3 and 2 mL HF (suprapure quality). Acid mineralisation was conducted using a CEM® Mars 6 microwave with iPrep vessels using the program "plant tissue". The heating protocol consisted of a 30 min ramp to 200 °C followed by a holding time of 10 min before cooling.

For the collected PM_{10} samples, half of the Teflon filter (previously weighed) was used and the PM_{10} were digested using the same acid mixture as for the plants. In this case, the "filter membrane" program was used, which consisted of a 30 min ramp until 200 °C followed by a holding time of 15 min before cooling.

All the obtained solutions were evaporated at 70 °C on a hotplate and the dry residues were resuspended in 0.37 N HNO_3 before analysis. Metal and metalloid concentrations in all diluted solutions (HNO_3 0.37N) were determined using inductively coupled plasma-mass spectrometry (ICP-MS) (iCAP Q Thermo Scientific®, from the ICP-MS Service of the Midi-Pyrénées Observatory in Toulouse, spiked with an In-Re internal standard to correct for instrumental drifts and plasma fluctuations; and from the ICP-MS AETE-ISO platform of OSU OREME, at the University of Montpellier, using Be, Sc, Ge, Rh and Ir as internal standards). Each batch of samples included an acid blank (or filter blank) and a certified reference material: SRM 1515 Apple leaves from the National Institute of Standards and Technology (NIST, USA) for *T. usneoides* samples and, SRM 1648a Urban particulate matter (NIST, USA) for the PM_{10} samples. Details on the quality of acid mineralisation, i.e. recoveries for the elements of SRM 1515 and SRM 1648a, are given in Supplementary Information (Table SI 2).

Details on the quality of the instrumental analyses, i.e. limits of detection (LOD) calculated as the average plus 3 times the standard deviation (SD) of the concentrations in the HNO_3 blanks, and recoveries for the elements of the instrumental SRMs: SRLS-6 (river water certified reference material for trace metals and other constituents) and EPOND (multi-element standard solution) are also given in Supplementary Information (Tables SI 3 and SI 4, respectively).

2.6. Atmospheric fallouts sourcing and environmental risk assessment

Enrichment factors (EF) and the pollution load index (PLI) were calculated to allow sources identification and risk assessment for the environment. In this study, the enrichment factors were considered to be indicative of the relative contribution of rock and soil dust to the elemental composition of *T. usneoides*. This is in view of the fact that emission of particles could potentially occur due to wind friction on surfaces. Enrichment factors were then calculated for each element by comparing their concentrations with the average upper crust (UC) composition reported by Rudnick and Gao (2003). Titanium (Ti) was chosen as the invariant for normalisation. This assumption is in accordance with the previous work by Delplace et al. (2022) who showed that the Ti content in the soils and sediments of the Orbiel valley has remained constant, with a $Ti/Ti_{upper\ crust}$ ratio close to 1. EF were calculated according to the formula:

$$EF = (Ci/CTi_{Tillandsia}) \div (Ci/CTi_{UC})$$

where Ci is the measured metal(loid) concentration, and CTi is the Ti concentration in the *T. usneoides* sample or in the upper crust (UC) (Pellegrini et al., 2014). In this study, EF values up to 10 are interpreted as indicative of a natural local dust origin from rock and soil, whereas higher EF values suggest input from sources other than rock and soil dust, potentially of anthropogenic origin. It should be noted that in EF calculations, the metal(loid) concentration (averaged over several specimens) in the unexposed plants was subtracted from the obtained concentration in the exposed plants. Even if the cut off value could be debated (Reimann and de Caritat (2005)), elements with EF > 10 are generally

considered to be enriched relative to their crustal abundances, and those with EF < 10 are considered non-enriched, as defined by Rahn (1976). This arbitrary cut off has been widely used by various authors including Dasch and Wolff (1989), Esmaeilirad et al. (2020), Freydier and Viers (2003), Gerdol et al. (2000), Pellegrini et al. (2004) and Veysseyre et al. (2001).

Finally, the PLI indicates the contribution of each metal(loid) to the global contamination of an area. The PLI, first proposed by Tomlinson et al. (1980) and recently used by Chen et al. (2022), was used to assess the environmental status of the different locations monitored by epiphytic plants. It was calculated by the following relationships:

$$Pi = Ci \div C_n^i$$

$$PLI = \sqrt[n]{\prod_i^n Pi}$$

where Pi is the single-factor pollution index, Ci are the measured metal(loid) concentrations in the exposed *T. usneoides* of the Orbiel valley, and C_n^i are the measured metal(loid) concentrations in the plants of control site of CBP for each of the exposure periods. According to the classification of Chen et al. (2022), the PLI values were then ranked in four levels, indicating no (PLI <1), mild (1 = PLI <2), moderate (2 = PLI <3), and severe pollution (PLI ≥3).

2.7. Statistical analyses

Statistical analyses were carried out using the R statistical software® 4.1.3. Given the size of the dataset and/or the non-normal distribution of the data, we used non-parametric Mann-Whitney tests to evaluate the statistical significance between the 9 exposure sites and the 4 exposure seasons. Non-parametric Spearman's rank correlations (denoted as R) were utilized to evaluate the strength of possible monotonic relationships between the different influencing factors, i.e., between elements and abiotic parameters, or between elements and the exposure time. P-values <0.05 were considered as statistically significant. Finally, PCA was done using the FactorMineR® package. Since the variables

were scaled in the PCA, replacing the missing data (values < LOD, representing 4 out of 60 values for the Tillandsia dataset and 6 out of 95 values for the PM_{10} dataset) by the average of the corresponding variables (for each specific location) should have no effect on PCA results. It should be noted that the results however, could be affected by outliers, since the PCA from FactoMineR is based on the Pearson's correlation coefficient matrix.

3. Results

In this study, we chose nine elements for analysis. Pb, As, Ni, Cd were investigated in view of their relevance to air quality standards regulations. In addition, we included elements that are indicative markers for different pollution sources such as dust (Ti, Fe), vehicle emissions (Cu, Sb, Cd), industrial activities (As, Cd, Pb, Zn), and fuel oil combustion (Ni) (Esmaeilirad et al. (2020)).

3.1. PM_{10} characterisation: mass concentration and elemental composition

The annual mass concentration values for PM_{10} collected in the Orbiel valley from Dec. 2021 to Dec. 2022 are reported in Figure 2 (A & B). It is seen that these values meet the European air quality standards (annual average 40 $\mu g.m^{-3}$) and there is no significant difference between the 4 sites. The average values for PM_{10} mass concentration are: 5.4, 6.1, 7.5 and 8.4 $\mu g.m^{-3}$ in CBP, MIR, LST and CDS, respectively. Moreover, the concentration in PM_{10}, all sites combined, was significantly higher in spring and lower in autumn 2022 (Figure 2 - B).

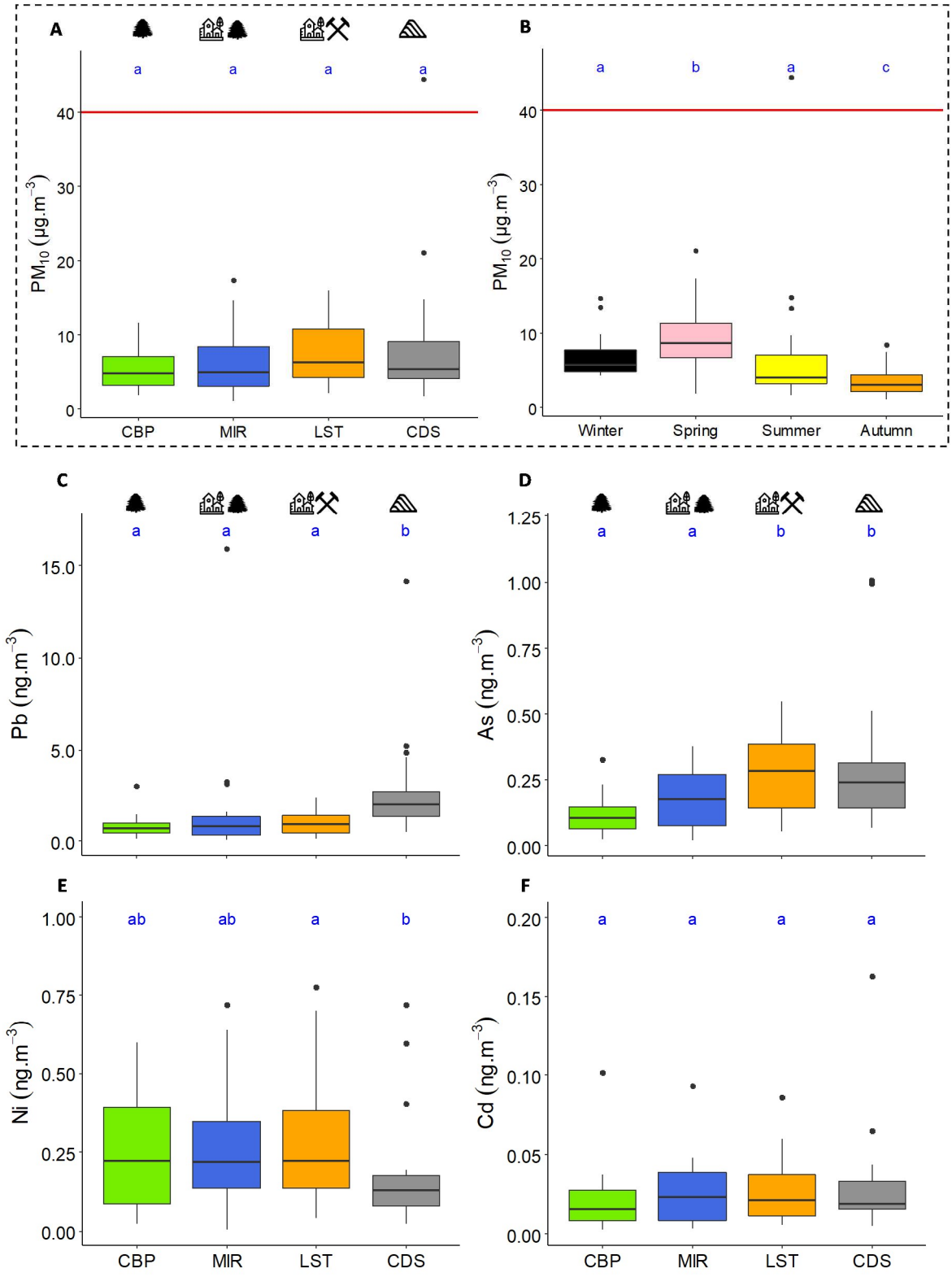

Figure 2: Mass concentrations of PM_{10} and of the metal(loid)s content in PM_{10} at the different investigated sites and over different seasons. *Top figures*: Annual PM_{10} mass concentrations (A) and seasonal distribution (B) of the PM_{10} concentrations (for all sites combined). *Bottom figures*: Elemental composition of Pb (C), As (D), Ni (E) and Cd (F). *Sites*: CBP = Gouffre de Cabrespine, MIR = Miraval, LST = Lastours, CDS = La Combe du Saut. *Red line = PM_{10} European air quality standards. Blue letters represent the statistical difference between sites or seasons (non-parametric Mann-Whitney tests).*

Data from PM_{10} impactors show that the annual mass concentration values for Pb, As, Ni and Cd meet the European air quality standards of 500, 6, 20 and 5 $ng.m^{-3}$, respectively (Figure 2 – C, D, E & F). Some differences were observed between the different sites for all elements except for Cd, which had a very low mass concentration in all the sites (average values of 0.02 in Gouffre de Cabrespine (CBP) to 0.03 $ng.m^{-3}$ for the other sites). For Pb, the mass concentration was significantly higher in La Combe du Saut site (CDS – average value of 2.8 $ng.m^{-3}$) than in the other sites (0.80 $ng.m^{-3}$ in CBP, 1.5 $ng.m^{-3}$ in Miraval (MIR) and 0.99 $ng.m^{-3}$ in Lastours (LST)). For As, the sites of LST (average value 0.27 $ng.m^{-3}$) and CDS (0.30 $ng.m^{-3}$) presented higher concentrations than the other sites (0.12 and 0.17 $ng.m^{-3}$ for CBP and MIR, respectively). Finally, the Ni concentration in LST (average value of 0.29 $ng.m^{-3}$) was significantly higher than in CDS (0.19 $ng.m^{-3}$), whereas CBP and MIR presented intermediate concentrations (0.26 and 0.27 $ng.m^{-3}$).

Concerning seasonal variations in Pb, As, Ni, and Cd mass concentrations, Ni exhibited the same trend as $PM_{10,}$ with higher concentrations in spring and reduced levels in autumn 2022. Pb, As, and Cd showed similar patterns: higher concentrations in winter/spring than in summer, with the lowest concentrations recorded in autumn (Figure SI 2).

3.1.1. Abiotic parameters' influence on PM_{10} concentration for the different sites

Figure 3 illustrates the behaviour of the five regulated pollutants (PM_{10}, As, Cd, Ni and Pb) with respect to different abiotic parameters; fitted lines are included to highlight trends. During the recorded period, the most frequent and strongest winds occurred from the northwest (Figure 3 A). Regarding these abiotic parameters, PM_{10}, As, Cd and Pb behaved similarly, but Ni showed a different trend, with increasing concentrations when the winds blew from the southwest direction, and decreasing concentrations when wind direction was from the east (Figure 3 B – zoomed figure is available in Figure

SI 3). Finally, a weak non-significant negative correlation was also found between PM_{10} mass concentration and precipitation (Figure 3 D).

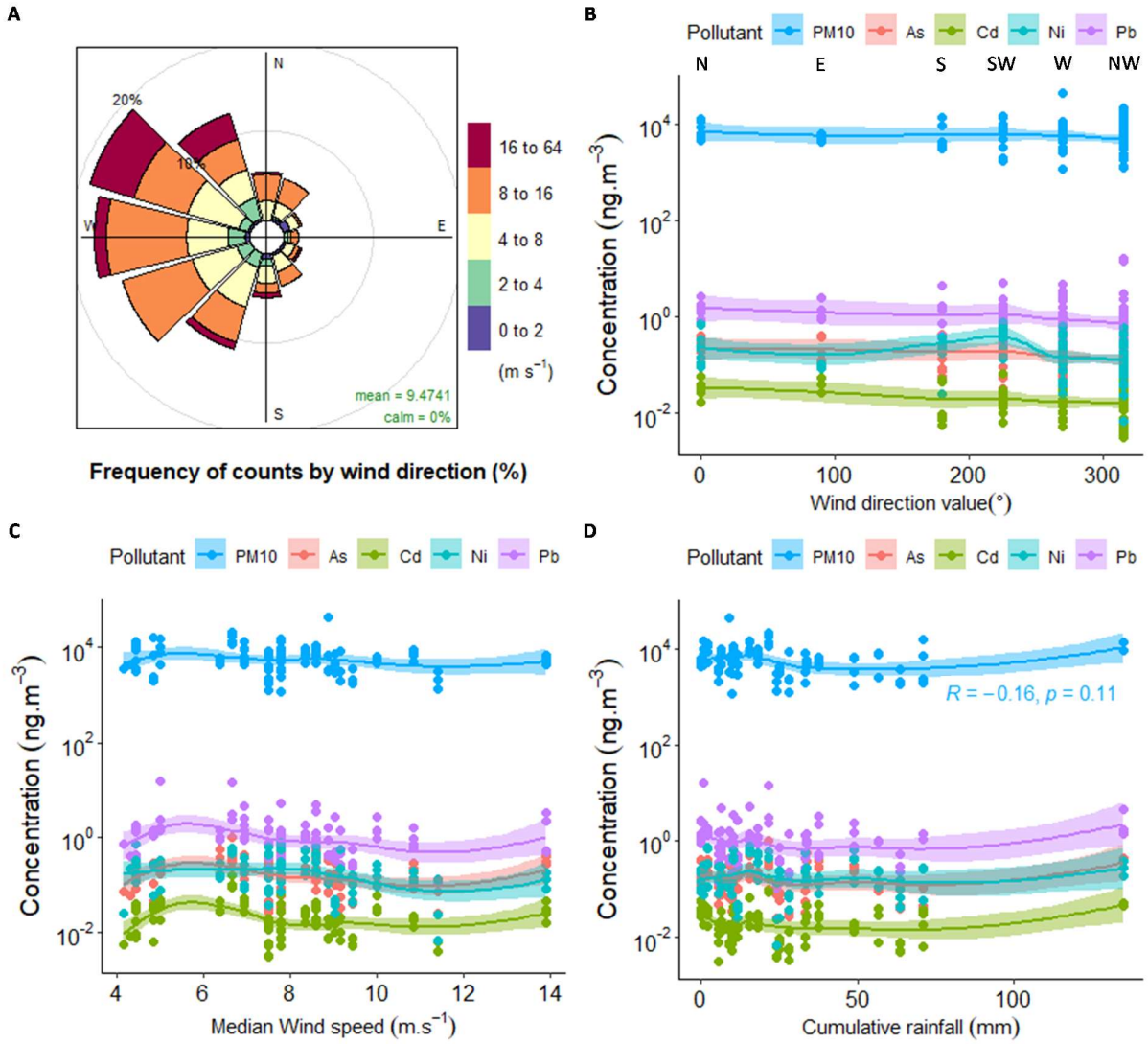

Figure 3: Abiotic parameters: Wind rose for the recorded period at the GPS point 43°20'52'' N, 2°23'29'' E (A), mass concentrations of PM_{10}, Pb, As, Ni and Cd with respect to wind direction (B), mean wind speed (C) and cumulative precipitation (D). *In graph (B), letters represent the wind direction. In graph (D), R = the strength of the linear relationship (Spearman correlation) and ρ= its statistical significance. For graphs (A, B, and C): trend lines have been added (LOESS smooth line).*

3.2. Tillandsia usneoides serve as biomonitors of metal(loid) composition of the atmosphere

As previously explained, the results presented here take into account, both adsorbed and potentially absorbed fractions. This is in line with our objective of not making a distinction between what remained on the plant surface and what was taken up by the plant tissue after atmospheric deposition.

3.2.1. SEM-EDX observations: atmospheric deposits on unexposed and exposed *T. usneoides*

SEM-EDX observations show the general morphology and the trichome structure in the shields of an unexposed *Tillandsia usneoides* (Figure 4-A&B). Contrastingly, the corresponding images of a plant exposed for 6 months at La Combe du Saut (CDS, Figure 4-C to F) show a homogeneous distribution of atmospheric depositions on the plant surface, with coarse particles (from 2.5 µm to 20 µm) along with numerous fine particles (< 2.5 µm) (Figure 4-D). A majority of the EDX spectra show the presence of Si and O, indicating possible deposition of quartz (SiO_2) (observations not shown). The spectrum shown in Figure 4-F however underlines the presence of O, Fe, Al and traces of Cu, Sn, Mn and Cr.

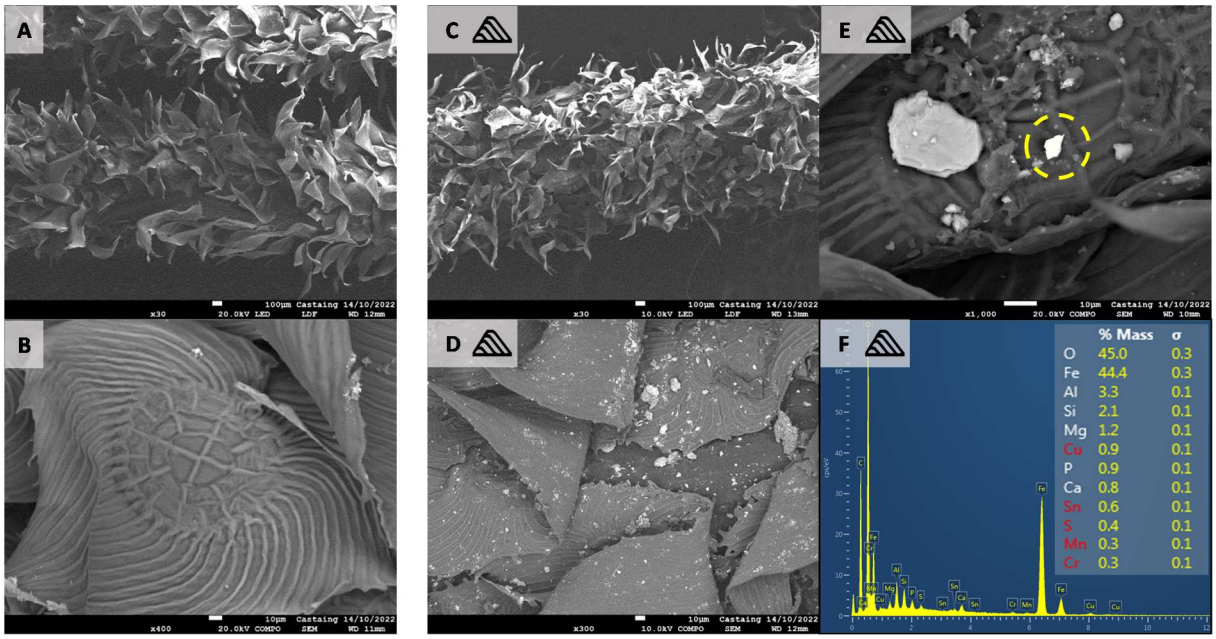

Figure 4: SEM-EDX observations of unexposed *(left images: A and B)* and *T. usneoides* exposed for 6 months *(right images: C, D, E and F)* at the site of La Combe du Saut (CDS). Overview of the unexposed plant (A), and trichomes structure (B). General observation of the exposed plant (C), Atmospheric deposits on the trichome structure (D), Atmospheric particle (surrounded in yellow) enriched in Fe and Al (according to the EDX spectrum) observed on a trichome (E and F).

3.2.2. Kinetics of atmospheric deposition (and potential uptake) by *T. usneoides*.

For most of the elements, the kinetics of atmospheric deposition on epiphytic plants (Figure 5) showed a linear increasing trend over a one-year period, with R values ranging from 0.56 (Pb and As) to 0.86 (Ti). On the other hand, a lower correlation between concentration and exposure time was observed for Cu, while no clear trend could be observed for Zn.

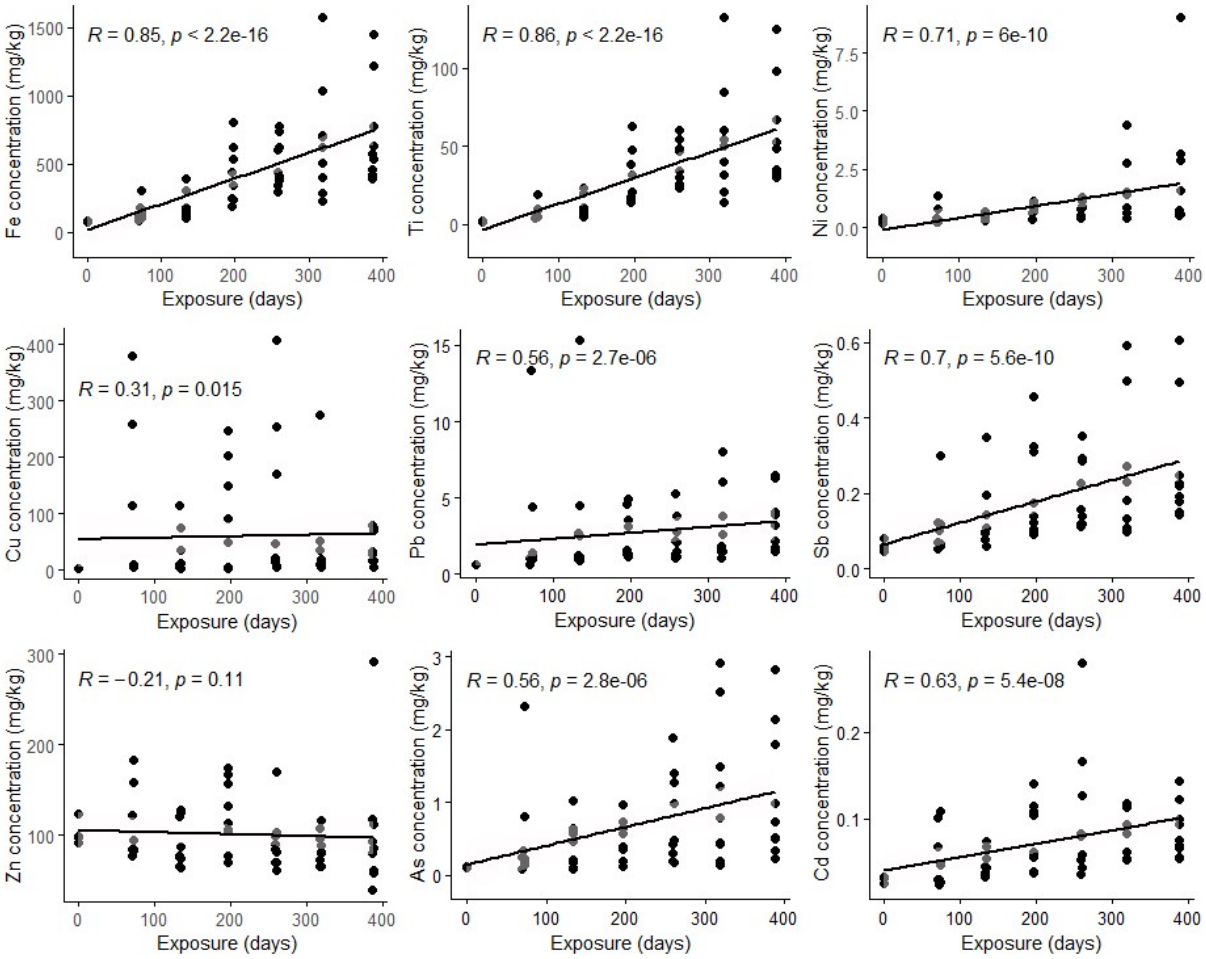

Figure 5: Atmospheric deposition over one year of exposure for the 9 considered elements. *R = strength of the linear relationship (Spearman) and ρ= its statistical significance.*

3.2.3. Effect of the location on elemental composition of *T. usneoides*

Figure 6 shows the metal(loid) concentrations in *T. usneoides* in the 9 investigated locations for the 9 target elements, without any discrimination of the exposure time. Data on all other elements can be found in the supporting information (Table SI 5). Significant differences are found between sites for As, Pb, Sb and Cd (Figure 6). A net distinction between sites can be made for As: the highest levels of this metalloid were found in MAL (Malabau), NRT (Nartau), GDL (Gué de Lassac) and CDS (La Combe du Saut), followed by CSO (Conques sur Orbiel), Lastours (LST) and Villanière (VLN). The lowest As concentrations were observed in plants positioned in MIR (Miraval) and Gouffre de Cabrespine (CBP),

387 which were at the same level as the unexposed (control) plants. For Pb, NRT and CDS sites but also
388 GDL, MIR and LST sites to a lesser extent, exhibited the highest concentrations in *T. usneoides.* For Sb
389 and Cd, the sites of Nartau (NRT), Gué de Lassac (GDL), and La Combe du Saut (CDS) presented higher
390 concentrations than the other sites.

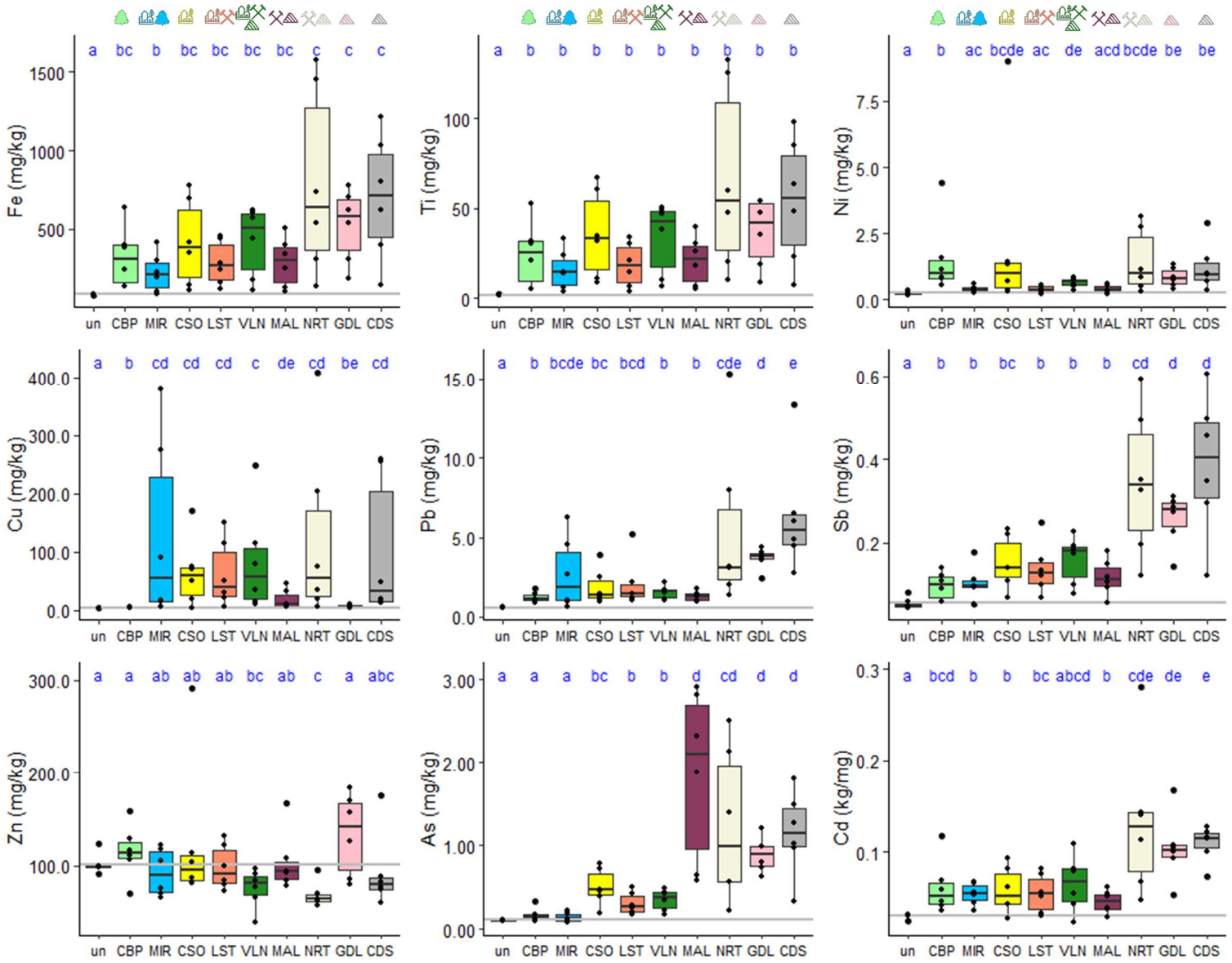

Figure 6: Elemental concentrations of Fe, Ti, Ni, Cu, Pb, Sb, Zn, As, and Cd (mg.kg^{-1}) in *T. usneoides* at the 9 studied sites from the Orbiel valley. un = unexposed plants; CBP = Gouffre de Cabrespine; MIR = Miraval; CSO = Conques sur Orbiel; LST= Lastours; VLN = Villanière; MAL = Malabau; NRT = Nartau; GDL = Gué de Lassac; CDS = La Combe du Saut. *Horizontal dotted line = mean for unexposed plants. Blue letters represent the statistical difference between sites (non-parametric Mann-Whitney tests).*

3.2.4. Evaluation of contamination levels and determination of atmospheric sources

Results of EF are reported in Figure 7. No significant enrichment in Fe and Ni (EF << 10) is indicated for the different studied locations, whereas enrichment in Cd, Sb and Zn is observed in all sites (except for VLN and NRT – no data). With the exception of CBP and GDL, all the locations present an enrichment in Cu. An enrichment in Pb is also observed for *T. usneoides* placed in the sites of MIR, LST, NRT, GDL and CDS (median EF values greater than 10). Finally, an enrichment in As is also observed in the plants exposed in MAL, NRT, GDL, and in LST sites to a lesser extent (median EF values greater than 10; see Figure 7).

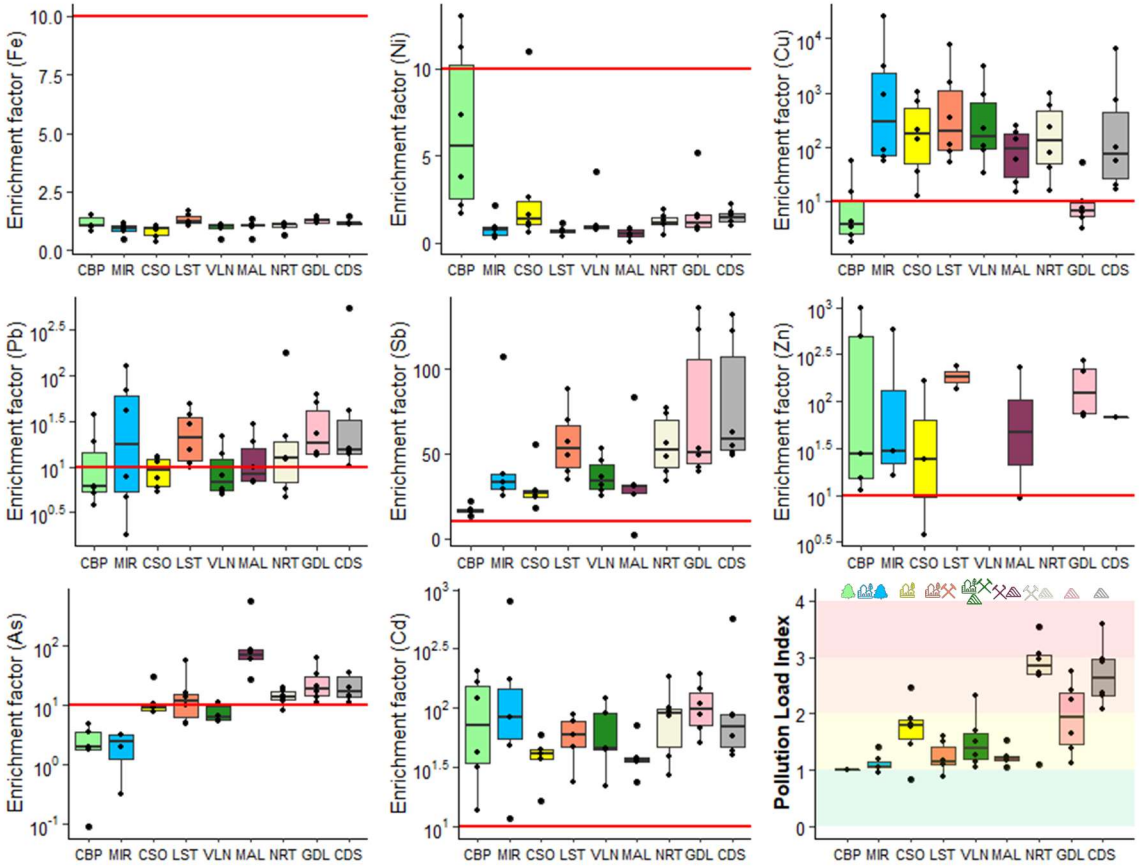

Figure 7: Indicators (EF and PLI) for environmental status assessment of the 9 studied sites of the Orbiel valley : CBP= Gouffre de Cabrespine; MIR= Miraval; CSO= Conques sur Orbiel; LST= Lastours; VLN= Villanière; MAL= Malabau; NRT= Nartau; GDL= Gué de Lassac; CDS= La Combe du Saut. **Enrichment factors (EF)** calculated **using crustal composition** (Rudnick and Gao, 2003) of the 8 elements of interest (except Ti) in *T. usneoides*. *Please note that a log scale is used except for Fe and Ni. The red line represents the threshold value EF = 10.* The **Pollution Load Index (PLI)** was calculated from *T. usneoides* data and from the concentrations of the 9 elements studied. *PLI <1 in green (no pollution), 1 = PLI <2 in yellow (mild pollution), 2 = PLI <3, in orange (moderate pollution), PLI ≥3 in red (severe pollution).*

The PCA results are reported in Figure 8, which highlight that 64.8 % of the variance contained in the data are retained by the first 2 principal components (PCs).

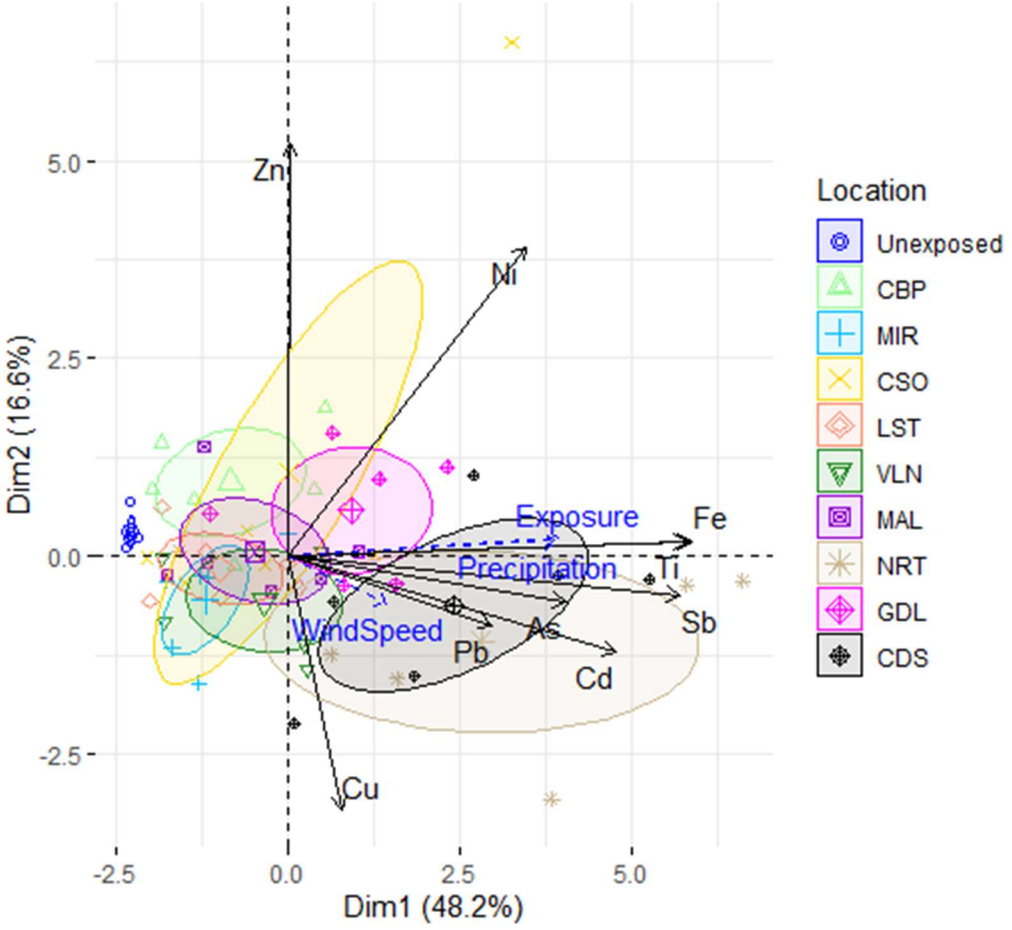

Figure 8: **PCA data results** for *T. usneoides*: biplot of individuals (samples) and variables (elements and abiotic parameters). CBP = Gouffre de Cabrespine; MIR = Miraval; CSO = Conques sur Orbiel; LST= Lastours; VLN = Villanière; MAL = Malabau; NRT = Nartau; GDL = Gué de Lassac; CDS = La Combe du Saut. *Note that the values of the axes represent the coordinates of individuals, not the variance.*

As shown in Figure SI 4, Fe, Ti, Sb, Zn, Ni and Cd emerge as the primary contributors to the PCs. Positively correlated variables include Fe, Ti, Sb, Cd and As, with Ni and Pb to a lesser extent. Additionally, negatively correlated variables (Zn and Cu) are observed in the orthogonal dimension. Thus, 3 groups of individuals are observed on the PC1 axe: (i) unexposed plants presenting low values for the 9 elements considered here; (ii) NRT and CDS locations displaying high values in Fe, Ti, Sb, Cd, As and Pb; and (iii) an intermediary group composed of the 7 other locations (CBP, CSO, GDL, LST, MAL, MIR, VLN).

3.2.5. Assessment of the environmental status with pollution index

The results of PLI calculations, performed while comparing the concentrations measured in plants from the control site of CBP, are shown in Figure 7 (bottom right). A mild pollution index is found for CBP, MIR, LST, MAL and GDL (median values: 1 = PLI <2) whereas a moderate pollution index is obtained for NRT and CDS (median values: 2 = PLI <3).

4. Discussion

4.1. Global air quality in the Orbiel valley

4.1.1. Assessment through PM_{10} atmospheric concentrations

The values of PM_{10} mass concentration and elemental composition measured in the present study are in accordance with previously reported data for the same area as described in two technical reports from the French geological survey (BRGM) in 2006 and 2020 (Bausch and Merlen, 2021; Durif et al., 2006).

The present results (obtained in 2022) in the Orbiel valley have also been compared to similar data on other sites in France and worldwide. Two French rural sites with and without industrial background have been used for comparison: the site of Peyrusse-Veille for the period of 2022, and the former metallurgical plant of Viviez for the period of 2021 (www.atmo-occitanie.org). In addition, two foreign rural sites with a mining history have also been considered for the comparison: the Nerva village site near the former Rio Tinto mine in Spain for the period of March 2009 – March 2010 (Sánchez de la Campa et al., 2011) and the Pitcher site near the "Chat" tailings of a former mine in the USA for the period of July 2005 –September 2006 (Zota et al., 2009). Overall, with a few exceptions, results for air quality in the Orbiel valley were better than those obtained in the 4 sites chosen for comparison. When comparing the French rural sites, we find that investigated locations in the Orbiel valley show lower concentrations of PM_{10}, Cd and Ni, than the other 2 French sites; for PM_{10}, the average values were 11

448 µg.m^{-3} in both Peyrusse-Vielle and Viviez. For Cd, and Ni, the corresponding values were 0.04 and 1
449 ng.m^{-3} and 0.45 and 0.40 ng.m^{-3} in Peyrusse Vielle and Viviez, respectively. The concentrations of As
450 were locally higher in the Orbiel valley (in CDS and LST) than in Peyrusse-Vielle (0.19 ng.m^{-3}), but lower
451 than that recorded at the Viviez site (0.40 ng.m^{-3}). Similarly, Pb concentrations were locally higher in
452 the Orbiel valley (in CDS and MIR) than in Peyrusse-Vielle (1.3 ng.m^{-3}), but lower or in the same range
453 as that recorded at the Viviez site (2.7 ng.m^{-3}). Overall, the concentrations (PM_{10}, Pb, As, Cd and Ni) in
454 the former mining sites in Spain and in the USA were higher than in the Orbiel valley, with the exception
455 of the Pitcher site where As values were < LOD, and undetermined for Cd and Ni.
456

457 4.1.2. Assessment through biomonitoring using *Tillandsia usneoides*

458 The metalloid concentrations in unwashed plants following exposure for 2 months in the Orbiel valley,
459 were compared with those on unwashed plants exposed for 36 days in a rural site near Pisa in Italy
460 (Pellegrini et al., 2014; rural/remote (RR) site), and with unwashed plants exposed for 8 weeks in two
461 traffic sites in the city of São Paulo in Brazil (Figueiredo et al., 2007; Cerqueira César (CC) and
462 Congonhas (CG) sites). This comparison allowed to assess the total atmospheric deposition depending
463 on the exposure site. Overall, among the eight elements compared, the concentrations of Ni, Cd, Fe
464 and Sb in the plants exposed in the Orbiel valley (average concentrations excluding the CBP site) were
465 lower than the corresponding values observed in plants exposed in a rural area in Italy (~ 8, 3, 2 and 2
466 times, respectively), or sites under dense traffic in the city of São Paulo (about 6 times for Fe and 7
467 times for Sb) (Table SI 6). It is worth noting that the values for Fe and Sb were higher at the GDL site
468 than at the rural site in Italy. With respect to the other 4 elements, the average concentration of Zn in
469 the Orbiel valley was in the same range as that in the rural site in Italy (around 100 mg.kg^{-1}) and was
470 1.6 times higher than in the traffic-ridden sites of São Paulo. Significantly, the average concentration
471 of Cu in the Orbiel valley after two months of exposure was 14 times higher than in the Italian site (no
472 data for São Paulo). Finally, for As and Pb, the average concentrations in the Orbiel valley were 2 times

473 higher than in the studied site in Italy (for both elements) and in the traffic-ridden sites in São Paulo
474 (1.4 times for As, no data for Pb in São Paulo) (Table SI 6).
475 Thus, although the Orbiel valley is home to a large number of mining sites, the resuspension of PM and
476 its deposition on *T. usneoides* appears to be limited.
477

478 4.2. Identification of potential sources of metal(loid) in the atmosphere

479 4.2.1. Source apportionment using abiotic parameters and PM_{10} trends

480 The concentrations of As, Cd, and Pb show similar behaviour with respect to wind direction, the median
481 wind speed and the cumulative rainfall, as well as the observed similarity in seasonal trend. This
482 strongly indicates that that these elements come from the same source and from similar atmospheric
483 processes (Figures 2 and 3). In their study on the influence of Saharan mineral dust on PM_{10}
484 concentration and composition in the city of Constantine (Algeria), Lokorai et al. (2021) reported that
485 a similarity in temporal evolution of the elements could indicate a common origin. In contrast, the
486 different seasonal behaviour of Ni and above all, its different behaviour in relation to the wind
487 direction, suggest that its source should be different from that of As, Cd and Pb (Figures SI 2 and SI 3).
488 The influence of the surface temperature was not examined further in view of the low concentrations
489 measured during summer 2022. Lastly, the frequent and strongest winds occurring from the
490 west/northwest direction were associated with air masses carrying rainfall (Figure SI 5). In fact, during
491 the sampling period, the valley experienced one extreme precipitation event (cumulated rain >100
492 mm) linked to southwardly winds, or "Cévenol event" (Figure SI 5). Our data indicate that this event
493 was also associated with a slight increase in atmospheric concentrations for PM_{10}, As, Pb, Ni and Cd
494 (Figure 3 D), but the overall precipitation data through one complete year, shows (Figure 3 D, R= –
495 0.16) a small decreasing trend for PM_{10} washout, suggesting that washout during rainfall was certainly
496 quite low. Thus, in this case, dry deposition by sedimentation seems to be the most efficient process
497 for coarse particles deposition (Grantz et al. 2003).

4.2.2. Atmospheric biomonitoring brings new insights to sources' tracing

The elemental composition of *T. usneoides* (Figure 6 and Table SI 5) allowed to identify the most exposed sites in the Orbiel valley and also to successfully identify the potential sources of air contamination in this valley. As already pointed out (section 4.1.2), the plants exposed in NRT, GDL and CDS sites had higher concentrations of Pb, Sb, As and Cd than those in the other places. The plants that were exposed close to the MAL site also had high levels of As. These 4 biomonitored sites were located near 4 of the 5 waste storages studied here.

Moreover, results of EF calculation for epiphytic plants (Figure 7) indicate that Ni and Fe (EF values << 10) were the non-enriched elements in this valley with a local rock and soil dust origin. On the other hand, the enriched elements in the valley (median EF values ≥ 10) were Cu, Zn, Sb and Cd, but also As and Pb for some sites. As reported in Figure 7, the MIR site shows an enrichment in Pb, while the MAL site presents the highest enrichment in As. Both elements appear as enriched in LST, as well as in NRT, GDL and CDS sites. We remind here that the sites of MAL, NRT, GDL and CDS were considered as the most exposed to mining activities in this valley including waste storage, old mining extractions and industries. This observation thus indicates inputs from sources other than the natural local rocks and soil dust, pointing to potential anthropogenic origins. However, in the Orbiel valley, there is a considerable natural enrichment of elements such as As in the geological bedrock, which provides a rationale for the intense extractive activities that occurred for centuries in this area. Therefore, instead of the average upper crust values, we used for comparison, the average local pedo-geochemical background (PGB) concentrations of the various metal(loid)s recently determined by Delplace and al. (2020) to recalculate the EF values. Results (Figure SI 6) illustrate that lower EF values were obtained, especially for As and Pb, indicating that in this area, the As and Pb content could be associated with resuspension of soil dusts due to local wind erosion. With regard to the enrichment in Pb in the MIR area (upstream part of the Orbiel river), it should be noted that Heydon et al. (2023) also identified the

highest Pb concentrations in the Orbiel river within this area. These results could be an indication that several ecosystems in this part of the valley could be contaminated with Pb.

To further link our results to potential sources, a PCA was performed (Figure 8). The 1st component accounted for 48.2% of the variance with a co-variance observed among several elements: Fe (10.3% of the total variance), Ti (10.1%), Sb (9.7%), Cd (6.8%), As (4.9%), and to a lesser extent, Ni and Pb (respectively, 3.6%, 2.6%) (see Figure SI 4 for more details). As an explanation, Fe, Ti and Ni were supposed to be associated to natural local rock and soil dust sources (as suggested by the EF values). On the other hand, Sb, Cd and As (and Pb), with EF values > 10, were supposed to be associated to possible anthropogenic sources. Finally, enrichment factors associated with the co-variation observed for the different elements indicate possible impact of dust and resuspension of anthropogenic materials sources (road, waste storage). To confirm this hypothesis, a PCA was done with PM_{10} data collected for the 4 monitored sites (Figure SI 7): 72.1% of the variance was retained in the first component (82.5 % for the first 2 components). The co-variation of all the elements, with the variables explaining from 9.1% (Zn) to 6.4% (Pb) of the variance, confirmed our previous finding from results on *T. usneoides*, that resuspensions of both dust and materials of anthropogenic origin, are the main sources of atmospheric contamination in the valley.

4.3. Assessment of the environmental status of the Orbiel valley

4.3.1. Indicators to assess the environmental status

Pollution load indexes calculated in epiphytic plants indicated a moderate contamination for NRT and CDS sites, and a mild pollution for the other locations (Figure 7). These PLI values are higher than those reported by Chen et al. (2022), who used pine needle as bioindicators of air quality and found none to mild pollution in different sites in Wuhan and Yichang. However, we note here that, different bioindicators and elements were selected in the two studies for the PLI calculations. In our case, PLI results are in accordance with our previous results, i.e., a moderate contamination was detected in the

548 valley using conventional instrumentation (PM_{10} results in accordance to EU standards) and
549 biomonitoring technique (low concentrations after 2 months of exposure when compared with values
550 reported in the literature), and the NRT and CDS sites (PLI and PCA results) were found to be the most
551 contaminated sites in the valley. Calculation of PLI has allowed to summarize this information, classify
552 the sites with respect to each other, and provided a simple way to assess the environment status of
553 the area.
554

555 ### 4.3.2. Using biomonitoring to better estimate chronic exposure

556 The kinetics of atmospheric fallouts on *Tillandsia* species have been reported in a few recent studies,
557 but the conclusions drawn have not been unanimous. Parente et al. (2023), assessed the air quality of
558 residential areas in the vicinity of the Brumadinho collapsed tailings dam in Brazil. They observed
559 higher concentrations of As, Ni and Hg in *T. usneoides* after 15 days than after 45 days of exposure,
560 suggesting a non-linear accumulation behaviour for these elements. However, a linear behaviour was
561 observed for Cr, Cu, Fe and Mn. Figueiredo et al. (2007) studied the urban area of São Paulo in Brazil,
562 and Martínez-Carrillo et al. (2010), in their investigation on the Tula–Tepeji industrial area in Central
563 Mexico, reported a maximal accumulation in *T. usneoides* after about 2 months of exposure. Isaac-
564 Olivé et al. (2012), also showed for the Tula–Tepeji industrial area (Central Mexico) that the
565 concentration of lanthanide elements reached a maximum after 10 weeks. Schreck et al. (2016), using
566 *Tillandsia capillaris* (in the mining district of Oruro, Bolivia), reported an almost linear response for As,
567 Cd, Hg, and Sn, but not for Ag, Pb, Sb, and Zn after 5 months of exposure. Finally, Schreck at al. (2020),
568 in their study on the old mining district of Cartagena-La Unión in Spain, observed a global increase in
569 Zn, Pb, As and Cd over time (12 months – *T. usneoides*).
570 In our study, we observe "strong" ($R > 0.5$) linear deposition up to 12 months of exposure for Fe, Ti, Ni,
571 Sb, Cd, Pb and As (Figure 5). This suggests that this plant species could be efficiently used under these
572 conditions of a former mining district and allows continuous monitoring of these elements over at least

one year. However, for Zn and Cu, such conclusions could not be made; these elements can be identified as nutrients. Moreover, it is interesting to mention that Martínez-Carrillo et al. (2010) observed low accumulation rates for elements such as Cu, Zn (and Fe) in *T. usneoides*, when comparing them to those on filters. Regarding Cu and Zn, results of our two PCAs did not converge, confirming our previous finding, that these micro-nutrients show a different response (non-linear deposition) when biomonitored with *T. usneoides*. The kinetics of atmospheric deposition on *Tillandsia* species over one year of exposure and with frequent inter-sampling periods have not been discussed in detail in these other studies (Figueiredo et al., 2007; Isaac-Olivé et al., 2012; Martínez-Carrillo et al., 2010; Parente et al., 2023; Schreck et al., 2016; Schreck et al., 2020). One plausible explanation for the variation in Cu and Zn behavior in *T. usneoides* could be the physicochemical properties of Cu- and Zn-bearing mineral particles (size, speciation and solubility) which might have led to their preferential leaching. The second explanation concerns physiological processes, i.e. differential uptake according to requirements or excretion/detoxification processes involving these elements (Schreck et al., 2016). In our study, dilution attributed to plant growth has been ruled out, as we do not see this effect on other elements. There is the case of Fe, a micro-nutrient, which presented a linear kinetics of deposition onto plants. We attribute this result to the presence of Fe (hydr)oxides (as indicated by SEM-EDX analyses, Figure 4) and the low solubility and bioavailability of these (hydr)oxides.

Despite 2022 being recorded as an unusual year with respect to climate with extreme climatic values and low precipitation, these epiphytic plants appear to be efficient indicators to follow air quality in the Orbiel valley. Moreover, due to climate change and global warming, extreme meteorological parameters will tend to be more generalised in our latitudes. This is particularly relevant since, as reported by Mandal et al. (2023), climate change can influence PM distribution and increase total $PM_{2.5}$ content in the atmosphere due to their longer lifetime, especially in summer.

Finally, in terms of chronic exposure and potential health risks through inhalation, it is worth citing WHO reports that mention that fine particle pollution has health impacts even at very low

599 concentrations, and there is no threshold below which no damage to health is observed (World Health
600 Organization, 2016). Our relatively simple, cheap and convenient approach could therefore be
601 generalised to understand chronic exposure to metal(loid) rich particles. Nevertheless, more research
602 is needed to extend biomonitoring to the other PM constituents (PAH, for example).
603

604 5. Conclusion

605 In 2022, the air quality in the Orbiel valley was found to be good, with PM_{10} levels in line with the EU
606 standards and in accordance with the two technical reports issued by the French geological survey
607 (BRGM) for the same area in 2006 and 2020. Moreover, the concentrations of detected elements in
608 the exposed plants were globally lower than the concentrations *on T. usneoides* reported in the
609 literature. Our different results, such as the influence of the abiotic parameters on PM_{10}
610 concentrations, PCAs results done on PM_{10} and *T. usneoides* data, as well as EF calculated in *T.*
611 *usneoides*, suggest that resuspensions of dust and of anthropogenic materials could be the sources of
612 most of the studied elements. Finally, the calculation of pollution indexes made it possible to
613 summarise the information, to classify the sites, and to identify Nartau and La Combe du Saut sites
614 (situated in waste storage and former mining industry area), as the most affected.
615 To fully understand the human exposure routes in the valley, more work is needed that involves i)
616 measuring the PM oxidative potential (OP) for the inhalation route, and ii) determining toxic elements
617 linked to atmospheric deposition in vegetables for the food route to assess the risks linked to these
618 deposits on food. An epidemiological study would also help to further understand the association
619 between different exposure routes and the potential health risks to the inhabitants.

Acknowledgments

This work was carried out under the framework of the "DiagnOSE" project, funded in part by the Region Occitanie Pyrénées – Méditerranée, France, and managed by INP Toulouse. This work was also supported by the CNRS INSU EC2CO program, through the PhytAsOrb project. Aude Calas (first author) was financially supported for 2 years by the DiagnOSE project. We thank Manuel Henry for his technical help in acidic mineralisation in the clean laboratory; Rémi Freydier and Léa Causse from the AETE-ISO Plateform of OSU OREME, at the University of Montpellier, and Camille Duquenoy from the Service ICP-MS at the Midi-Pyrénées Observatory of Toulouse, for their assistance with ICP-MS analyses. We also express our gratitude to our colleague Stéphane Le Blond du Plouy from the Centre de Micro Caractérisation Raimond Castaing in Toulouse for his technical support in SEM-EDX analysis of *T. usneoides* and Dr. Revathi Bacsa for editorial assistance. Finally, this study could not have been conducted without the precious help and technical support for our atmosphere experiments from the local population, and especially Gilles Marty.

References

Bausch, P., Merlen, R., 2021. Etude des poussières atmosphériques dans le district minier de la vallée de l'Orbiel (11). Rapp. d'étude EVADIES - BRGM 1–147.

Blondet, I., Schreck, E., Viers, J., Casas, S., Jubany, I., Bahí, N., Zouiten, C., Dufréchou, G., Freydier, R., Galy-Lacaux, C., Martínez-Martínez, S., Faz, A., Soriano-Disla, M., Acosta, J.A., Darrozes, J., 2019. Atmospheric dust characterisation in the mining district of Cartagena-La Unión, Spain: Air quality and health risks assessment. Sci. Total Environ. 693. https://doi.org/10.1016/j.scitotenv.2019.07.302

Bondu, R., Casiot, C., Pistre, S., Batiot-Guilhe, C., 2023. Impact of past mining activities on water quality in a karst area in the Cévennes region, Southern France. Sci. Total Environ. 873. https://doi.org/10.1016/j.scitotenv.2023.162274

Chen, M., Lu, W., Hou, Z., Zhang, Y., Jiang, X., Wu, J., 2017. Heavy metal pollution in soil associated with a large-scale cyanidation gold mining region in southeast of Jilin, China. Environ. Sci. Pollut. Res. 24, 3084–3096. https://doi.org/10.1007/s11356-016-7968-3

Chen, Y., Ning, Y., Bi, X., Liu, J., Yang, S., Liu, Z., Huang, W., 2022. Pine needles as urban atmospheric pollution indicators: Heavy metal concentrations and Pb isotopic source identification. Chemosphere 296, 134043. https://doi.org/10.1016/j.chemosphere.2022.134043

Csavina, J., Field, J., Taylor, M.P., Gao, S., Landázuri, A., Betterton, E.A., Sáez, A.E., 2012. A review on the importance of metals and metalloids in atmospheric dust and aerosol from mining operations. Sci. Total Environ. 433, 58–73. https://doi.org/10.1016/j.scitotenv.2012.06.013

Dasch, J.M., Wolff, G.T., 1989. Trace inorganic species in precipitation and their potential use in source apportionment studies. Water. Air. Soil Pollut. 43, 401–412. https://doi.org/10.1007/BF00279205

de Fleury, M., Kergoat, L., Grippa, M., 2023. Hydrological regime of Sahelian small waterbodies from combined Sentinel-2 MSI and Sentinel-3 Synthetic Aperture Radar Altimeter data. Hydrol. Earth Syst. Sci. 27, 2189–2204. https://doi.org/10.5194/hess-27-2189-2023

Delplace, G., Viers, J., Schreck, E., Oliva, P., Behra, P., 2022. Pedo-geochemical background and sediment contamination of metal(loid)s in the old mining-district of Salsigne (Orbiel valley, France). Chemosphere

287. https://doi.org/10.1016/j.chemosphere.2021.132111

Desaulty, A., Négrel, P., Kloppmann, W., Petelet-Giraud, E., Gaboriau, H., 2016. Diagnostic multi-isotopique sur le site de La Combe du Saut (district de Salsigne - Aude). Rapp. Final BRGM/RP-65, p.69.

Drouhot, S., Raoul, F., Crini, N., Tougard, C., Prudent, A.S., Druart, C., Rieffel, D., Lambert, J.C., Tête, N., Giraudoux, P., Scheifler, R., 2014. Responses of wild small mammals to arsenic pollution at a partially remediated mining site in Southern France. Sci. Total Environ. 470–471, 1012–1022. https://doi.org/10.1016/j.scitotenv.2013.10.053

Durif, M., Fable, S., Gay, G., Karoski, N., Meunier, L., Tack, K., 2006. Evaluation quantitative des risques sanitaires liés à l ' inhalation des particules métalliques issues des sols de surface par les populations riveraines du site d ' exploitation minier du site. Rapp. d'étude Ineris 26.

Elbaz-Poulichet, F., Resongles, E., Bancon-Montigny, C., Delpoux, S., Freydier, R., Casiot, C., 2017. The environmental legacy of historic Pb-Zn-Ag-Au mining in river basins of the southern edge of the Massif Central (France). Environ. Sci. Pollut. Res. 24, 20725–20735. https://doi.org/10.1007/s11356-017-9669-y

Esmaeilirad, S., Lai, A., Abbaszade, G., Schnelle-Kreis, J., Zimmermann, R., Uzu, G., Daellenbach, K., Canonaco, F., Hassankhany, H., Arhami, M., Baltensperger, U., Prévôt, A.S.H., Schauer, J.J., Jaffrezo, J.L., Hosseini, V., El Haddad, I., 2020. Source apportionment of fine particulate matter in a Middle Eastern Metropolis, Tehran-Iran, using PMF with organic and inorganic markers. Sci. Total Environ. 705, 135330. https://doi.org/10.1016/j.scitotenv.2019.135330

Figueiredo, A.M.G., Nogueira, C.A., Saiki, M., Milian, F.M., Domingos, M., 2007. Assessment of atmospheric metallic pollution in the metropolitan region of São Paulo, Brazil, employing Tillandsia usneoides L. as biomonitor. Environ. Pollut. 145, 279–292. https://doi.org/10.1016/j.envpol.2006.03.010

Freydier, R., Viers, J., 2003. Isotopic study of lead transfer at the interface soil-plants-atmosphere. Geophys. Res. Lett. 30, 1–4. https://doi.org/10.1029/2002GL016145

Gerdol, R., Bragazza, L., Marchesini, R., Alber, R., Bonetti, L., Lorenzoni, G., Achilli, M., Buffoni, A., De Marco, N., Franchi, M., Pison, S., Giaquinta, S., Palmieri, F., Spezzano, P., 2000. Monitoring of heavy metal deposition in Northern Italy by moss analysis. Environ. Pollut. 108, 201–208. https://doi.org/10.1016/S0269-7491(99)00189-X

Grantz, D.A., Garner, J.H.B., Johnson, D.W., 2003. Ecological effects of particulate matter. Environ. Int. 29, 213–239. https://doi.org/10.1016/S0160-4120(02)00181-2

Heydon, M., Perez Serrano, L., Schreck, E., Causserand, C., Pokrovsky, O.S., Behra, P., Viers, J., 2023. Role of colloids in the transfer and dispersion of trace elements into river waters through a former mining district. Appl. Geochemistry 155, 105736. https://doi.org/10.1016/j.apgeochem.2023.105736

Huertas, J.I., Huertas, M.E., Izquierdo, S., González, E.D., 2012. Air quality impact assessment of multiple open pit coal mines in northern Colombia. J. Environ. Manage. 93, 121–129. https://doi.org/10.1016/j.jenvman.2011.08.007

Isaac-Olivé, K., Solís, C., Martínez-Carrillo, M.A., Andrade, E., López, C., Longoria, L.C., Lucho-Constantino, C.A., Beltrán-Hernández, R.I., 2012. Tillandsia usneoides L, a biomonitor in the determination of Ce, La and Sm by neutron activation analysis in an industrial corridor in Central Mexico. Appl. Radiat. Isot. 70, 589–594. https://doi.org/10.1016/j.apradiso.2012.01.007

Khaska, M., Le Gal La Salle, C., Verdoux, P., Boutin, R., 2015. Tracking natural and anthropogenic origins of dissolved arsenic during surface and groundwater interaction in a post-closure mining context: Isotopic constraints. J. Contam. Hydrol. 177–178, 122–135. https://doi.org/10.1016/j.jconhyd.2015.03.008

Lokorai, K., Ali-Khodja, H., Khardi, S., Bencharif-Madani, F., Naidja, L., Bouziane, M., 2021. Influence of mineral dust on the concentration and composition of PM10 in the city of Constantine. Aeolian Res. 50, 100677. https://doi.org/10.1016/j.aeolia.2021.100677

Mandal, M., Das, S., Roy, A., Rakwal, R., Jones, O.A.H., Popek, R., Agrawal, G.K., Sarkar, A., 2023. Interactive relations between plants, the phyllosphere microbial community, and particulate matter pollution. Sci. Total Environ. 890, 164352. https://doi.org/10.1016/j.scitotenv.2023.164352

Martínez-Carrillo, M.A., Solís, C., Andrade, E., Isaac-Olivé, K., Rocha, M., Murillo, G., Beltrán-Hernández, R.I., Lucho-Constantino, C.A., 2010. PIXE analysis of Tillandsia usneoides for air pollution studies at an industrial zone in Central Mexico. Microchem. J. 96, 386–390. https://doi.org/10.1016/j.microc.2010.06.014

Parente, C.E.T., Carvalho, G.O., Lino, A.S., Sabagh, L.T., Azeredo, A., Freitas, D.F.S., Ramos, V.S., Teixeira, C., Meire, R.O., Ferreira Filho, V.J.M., Malm, O., 2023. First assessment of atmospheric pollution by trace elements and particulate matter after a severe collapse of a tailings dam, Minas Gerais, Brazil: An insight into

biomonitoring with Tillandsia usneoides and a public health dataset. Environ. Res. 233. https://doi.org/10.1016/j.envres.2023.116435

Pellegrini, E., Lorenzini, G., Loppi, S., Nali, C., 2014. Evaluation of the suitability of Tillandsia usneoides (L.) L. As biomonitor of airborne elements in an urban area of Italy, Mediterranean basin. Atmos. Pollut. Res. 5, 226–235. https://doi.org/10.5094/APR.2014.028

Rahn, K. A., 1976. The Chemical Composition of the Atmospheric Aerosol. Graduate School of Oceanography, University of Rhode Island.

Reimann, C., De Caritat, P., 2005. Distinguishing between natural and anthropogenic sources for elements in the environment: Regional geochemical surveys versus enrichment factors. Sci. Total Environ. 337, 91–107. https://doi.org/10.1016/j.scitotenv.2004.06.011

Rochereau, F., Albinet, R., Labastie, A., Huron, Y., Vaxélaire, S., Rivet, F., Nedellec, J., 2021. Anciens sites miniers et industriels de la vallée de l'Orbiel (11) Rapport annuel de surveillance 2020. Rapp. Final BRGM BRGM/RP-71, 195.

Rudnick, R.L., Gao, S., 2003. Composition of the Continental Crust. Treatise on Geochemistry 3, 64. https://doi.org/10.1016/B0-08-043751-6/03016-4

Sánchez de la Campa, A.M., de la Rosa, J.D., Fernández-Caliani, J.C., González-Castanedo, Y., 2011. Impact of abandoned mine waste on atmospheric respirable particulate matter in the historic mining district of Rio Tinto (Iberian Pyrite Belt). Environ. Res. 111, 1018–1023. https://doi.org/10.1016/j.envres.2011.07.001

Schreck, E., Sarret, G., Oliva, P., Calas, A., Sobanska, S., Guédron, S., Barraza, F., Point, D., Huayta, C., Couture, R., Prunier, J., Henry, M., Tisserand, D., Goix, S., Chincheros, J., Uzu, G., 2016. Is Tillandsia capillaris an efficient bioindicator of atmospheric metal and metalloid deposition ? Insights from five months of monitoring in an urban mining area. Ecol. Indic. 67, 227–237. https://doi.org/10.1016/j.ecolind.2016.02.027

Schreck, E., Viers, J., Blondet, I., Auda, Y., Macouin, M., Zouiten, C., Freydier, R., Dufréchou, G., Chmeleff, J., Darrozes, J., 2020. Tillandsia usneoides as biomonitors of trace elements contents in the atmosphere of the mining district of Cartagena-La Unión (Spain): New insights for element transfer and pollution source tracing. Chemosphere 241. https://doi.org/10.1016/j.chemosphere.2019.124955

Tepanosyan, G., Sahakyan, L., Belyaeva, O., Asmaryan, S., Saghatelyan, A., 2018. Continuous impact of mining activities on soil heavy metals levels and human health. Sci. Total Environ. 639, 900–909. https://doi.org/10.1016/j.scitotenv.2018.05.211

Tomlinson, D.L., Wilson, J.G., Harris, C.R., Jeffrey, D.W., 1980. Problems in the assessment of heavy-metal levels in estuaries and the formation of a pollution index. Helgoländer Meeresuntersuchungen 33, 566–575. https://doi.org/10.1007/BF02414780

Trueb, L.F., 1996. The salsigne gold mine: A world-class ore body in the south west of France. Gold Bull. 29, 137–140. https://doi.org/10.1007/BF03214749

Vermeersch, F., Labebvre, O., Vachette, C., 2012. Exploitations minières sur le secteur de Salsigne. Concessions de Malabau, Pujol, Lastours,La Caunette, Salsigne, Villanière, Villardonnel . Evaluation et cartographie des aléas mouvements de terrain. Rapp. synthèse Géoderis 39.

Veysseyre, A., Moutard, K., Ferrari, C., Velde, K. Van de, Barbante, C., Cozzi, G., Capodaglio, G., Boutron, C., 2001. Heavy metals in fresh snow collected at different altitudes in the Chamonix and Maurienne valleys, French Alps: Initial results. Atmos. Environ. 35, 415–425. https://doi.org/10.1016/S1352-2310(00)00125-4

World Health Organization, 2021. WHO global air quality guidelines. Guidelines 1–360.

World Health Organization, 2016. Ambient air pollution: a global assessment of exposure and burden of disease. Rapport 1–131.

Yulevitch, G., Danon, M., Krasovitov, B., Fominykh, A., Swet, N., Tsesarsky, M., Katra, I., 2020. Evaluation of wind-induced dust-PM emission from unpaved roads varying in silt content by experimental results. Atmos. Pollut. Res. 11, 261–268. https://doi.org/10.1016/j.apr.2019.10.010

Zota, A.R., Willis, R., Jim, R., Norris, G.A., Shine, J.P., Duvall, R.M., Schaider, L.A., Spengler, J.D., 2009. Impact of mine waste on airborne respirable particulates in Northeastern Oklahoma, United States. J. Air Waste Manag. Assoc. 59, 1347–1357. https://doi.org/10.3155/1047-3289.59.11.1347